

Metric Space Magnitude for Evaluating the Diversity of Latent Representations

Katharina Limbeck^{*12} Rayna Andreeva^{*3} Rik Sarkar³ Bastian Rieck¹²

Abstract

The *magnitude* of a metric space is a recently-established invariant, providing a measure of the ‘effective size’ of a space across multiple scales while also capturing numerous geometrical properties. We develop a family of magnitude-based measures of the intrinsic diversity of latent representations, formalising a novel notion of dissimilarity between magnitude functions of finite metric spaces. Our measures are provably stable under perturbations of the data, can be efficiently calculated, and enable a rigorous multi-scale comparison of latent representations. We show the utility and superior performance of our measures in an experimental suite that comprises different domains and tasks, including the evaluation of diversity, the detection of mode collapse, and the evaluation of generative models for text, image, and graph data.

1. Introduction

Diversity is a key concept in representation learning, referring to the relative abundance and distinctiveness of model outputs. Given the increasing complexity of deep learning models, the evaluation of diversity is thus a critical task, enabling (i) the assessment of the *intrinsic richness* of latent representations, and (ii) the evaluation of the extent to which models are capable of *preserving* the properties of an input distribution. While the quantitative evaluation of generative models in particular relies on assessing trade-offs between fidelity and diversity with regards to a *known* reference distribution, reference-free diversity measures are becoming increasingly relevant when a ground-truth distribution is unknown or intractable. However, reference-based diversity metrics such as *recall* are notoriously fallible, whereas reference-free diversity measures often rely on simple mean summaries that lack expressivity to fully capture what it means for a space to be diverse (Friedman & Dieng, 2023). Defining an expressive measure of diversity requires entropy, category theory, and extended notions of

measures of *size* (Leinster, 2021). There is thus a critical need for novel measures that are theoretically motivated, robust to noise, and capable of encoding the intrinsic diversity of data across varying levels of similarity rather than at a single fixed threshold.

Our contributions. Addressing this need, we propose a novel family of diversity measures based on *metric space magnitude*, a mathematical invariant that captures numerous important multi-scale geometric characteristics of metric spaces, including curvature, density, and the diameter of an input space. Metric space magnitude merely requires a notion of dissimilarity between data points, permitting it to operate on both *local* and *global* scales. Hence, magnitude is poised to compare latent spaces, yielding a compact holistic summary of diversity that is inherently aware of geometric structures across multiple scales. Our work is the first to (i) formally introduce magnitude as a general tool for evaluating the diversity of latent representations, and (ii) formalise a notion of difference between the magnitude of two spaces across multiple scales of similarity. We demonstrate that magnitude is stable and can detect curvature, highlighting its use as a multi-scale summary of the local and global geometry of data. Moreover, we empirically showcase the utility of our magnitude-based diversity measure across different data modalities, namely text, image, and graph embeddings, for which we observe that our measure outperforms alternative embedding-based measures of intrinsic diversity. Finally, when a reference distribution is known, our magnitude-based notion of difference reliably detects *mode collapse* and *mode dropping*, thus assisting practitioners in model evaluation and selection.

2. Related Work

Latent representations and embeddings have become inevitable tools for analysing popular types of data, such as images, text, and graphs. As evidenced by LLMs, understanding semantic relationships in data requires meaningful embeddings, i.e. latent representations. Our work focuses on improving representation-based diversity evaluation and we thus consider the role diversity plays in this context.

2.1. Diversity Measures

The assessment of generative model diversity remains a daunting task irrespective of the domain (Theis et al., 2016),

^{*}Equal contribution ¹Helmholtz Munich ²Technical University of Munich ³University of Edinburgh. Correspondence to: Bastian Rieck <bastian.rieck@tum.de>.

since ground truth reference distributions or labelled data are often unavailable, and human evaluation remains costly. Thus, there exist a need for interpretable, automated and unsupervised measures of intrinsic diversity. While clearly applicable across varied modalities, this is of particular importance for assessing generated text given the high-universal use and black-box-nature of LLMs (Celikyilmaz et al., 2020). Motivated by this, a varied collection of diversity measures has been proposed, many of which are task-, domain- or model-specific (Friedman & Dieng, 2023); only a fraction of them are applicable to analysing latent representations specifically. The most flexible methods summarise intrinsic diversity using average pairwise dissimilarities like L^p distances or BERT-scores (Tevet & Berant, 2021). More recently, Friedman & Dieng (2023) proposed the Vendi Score, inspired by principles from theoretical ecology. Other diversity measures are computed directly on embedding spaces, using e.g. the geometric mean of the standard deviation across each embedding dimension (Lai et al., 2020) or cluster-based measures (Du & Black, 2019). However, as we explore in Section 3.1, none of these measures satisfy all theoretical guarantees required by an axiomatic approach to diversity, and they are limited in expressivity, providing only snapshots of diversity at a single fixed resolution.

Reference-based metrics define diversity as the extent to which generated samples cover the full variability of the real data (Naeem et al., 2020). Examples include the Fréchet Inception Distance (FID) or the Inception score (IS). However, they do not exclusively measure diversity but are also concerned with evaluating fidelity, i.e. the extent to which generated data resemble real data, making it unclear how single-number summaries such as FID and IS account for each aspect in the trade-off between diversity and quality. Thus, *precision* and *recall* have been suggested as more informative summary metrics (Sajjadi et al., 2018). Further improvements to these metrics have been suggested (Kynkäänniemi et al., 2019; Naeem et al., 2020; Simon et al., 2019). Unfortunately, as Naeem et al. (2020) show, even the improved versions of precision and recall fail to satisfy the useful conditions for strong evaluation metrics, such as (i) detecting identical reference and generated distributions, (ii) capturing mode dropping, and (iii) simplicity in selecting hyperparameters. To address these concerns, *density* and *coverage* have been proposed (Naeem et al., 2020). Nevertheless, these metrics still rely on manifold approximations to assess diversity, which makes them sensitive to parameter choices. By contrast, our magnitude-based measures have less stringent assumptions and can be defined in a parameter-free fashion.

2.2. Magnitude in Machine Learning

Since its introduction to measure biological diversity (Sollow & Polasky, 1994), magnitude has received a strong formalisation by Leinster (2013) in terms of category theory, leading to a comprehensive study of its mathematical characteristics (Leinster, 2021). Nevertheless, despite strong geometric properties, magnitude has only rarely been applied in a machine learning context, with recent publications starting to bridge this gap, linking magnitude to boundary detection (Bunch et al., 2021), edge detection in images (Adamer et al., 2021), or even the generalisation error of neural networks (Andreeva et al., 2023). Further, the close ties of magnitude to diversity have been exploited by Huntsman (2023) to maximise diversity in multi-objective optimisation. Nevertheless, the full potential of magnitude for measuring diversity remains unexplored since existing works ignore the nature of magnitude as an *intrinsic multi-scale summary*, which captures both local and global geometry and diversity of the data manifold. Our work is thus the first to leverage magnitude as a flexible, multi-scale indicator of diversity in latent representations.

3. Methods

We first discuss the theoretical properties a suitable diversity measure should satisfy and then introduce metric space magnitude. Based on this, we outline our proposed method using magnitude for measuring the diversity of latent representation and its practical implementation.

3.1. Desiderata for Diversity Measures

Given the difficulty in defining diversity, diversity metrics never measure diversity itself, but rather quantify related ideas. Entropy-based approaches, including magnitude, in particular share close links to diversity, often favoured in ecology for their computational benefits and agreement with fundamental axioms of diversity (Daly et al., 2018). Following this axiomatic approach, we highlight the following key requirements (Leinster, 2021):

- *Monotonicity in observations*: Including a new observation does not decrease diversity.
- *Monotonicity in distances*: Diversity does not decrease as the distance between observations increases.
- *Twin property*: Including a duplicate observation already in the set does not change diversity.
- *Continuity in similarity*: Diversity is a continuous function of the degree of similarity.
- *Absence invariant*: Diversity is invariant under the absence of observations.

This list is not conclusive; Appendix D.3 provides a more rigorous discussion of further properties.

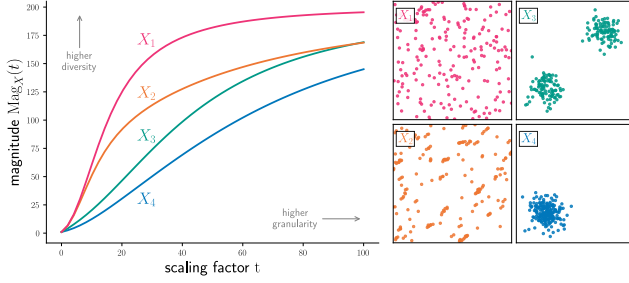


Figure 1. Example of magnitude functions for four metric spaces with 200 points, varying in diversity. The more diverse the space, the higher the value of its magnitude function. The scale factor t influences the degree of detail or granularity at which points are distinguished. When the scale factor t is very small, e.g. $t = 0.01$, magnitude is very close to 1, and each space effectively looks like one point. For large t , the number of effective points is noticeably higher and it is clear that X_1 is more diverse than X_2 , X_3 , and X_4 , respectively. Each magnitude function eventually converges to the cardinality of the input space.

Nevertheless, many baseline diversity measures for evaluating representations in ML already fail at the aforementioned requirements. Average similarity (AVGSIM) neither satisfies the twin property nor monotonicity in observations. Further, it simply gives a mean summary, which cannot capture nuances in diversity and fails even in simple toy scenarios (Friedman & Dieng, 2023). Similarly, the geometric mean of the standard deviations across each embedding dimension (Lai et al., 2020, GMSTDS) fails at these same conditions. Moreover, it is *not* invariant to the absence of observations. Despite being a more purpose-built diversity measure, the Vendi Score (VS), calculated as the exponential of the Shannon entropy of the eigenvalues of a normalised similarity matrix, is not monotone in observations either (Leinster, 2021). This axiomatic discussion on diversity thus points towards a glaring need for more principled diversity measures. Extending this discussion to reference-based evaluation, coverage-based approaches miss out on assessing the specific changes in intrinsic diversity, which we argue should also be evaluated in isolation. As we will show next, *magnitude functions* are particularly promising candidates for improved diversity measures that inherently satisfy all desiderata listed above.

3.2. The Magnitude of a Metric Space

Magnitude is an invariant that measures diversity by describing the ‘effective number of points’ of a metric space as a function of its scaled distances (Leinster, 2013).

Definition 3.1 (Magnitude of a metric space). Let $X = \{x_1, \dots, x_n\}$ be a finite metric space with an associated distance metric d . The *similarity matrix* of X is defined as $\zeta_X(i, j) := \exp(-d(i, j))$ for $1 \leq i, j \leq n$. If ζ_X is

invertible, the *magnitude* of X is defined as

$$\text{Mag}(X) := \sum_{ij} (\zeta_X^{-1})_{ij}. \quad (1)$$

The existence of magnitude is contingent on the existence of ζ_X . Given a *negative definite metric* d , such as the L^1 and L^2 distance, ζ_X is invertible (Feragen et al., 2015). Subsequently, we will assume that (X, d) with $X \subseteq \mathbb{R}^D$ permits the calculation of magnitude; in particular X must *not* have any duplicate points. While the magnitude of a metric space is expressive even at a *single* scale (Bunch et al., 2021; Leinster, 2013; Leinster & Shulman, 2021), magnitude unleashes its full potential in a *multi-scale* setting, assigning to a metric space not just a scalar but a function. To this end, we introduce a parameter $t \in \mathbb{R}_+$ and consider the metric space with distances scaled by t , which we denote by tX . Intuitively, this procedure corresponds to viewing the same space through different lenses, or at different ‘zoom factors,’ for example by converting distances from metres to centimetres. Computing the magnitude for each value of t then yields the *magnitude function*.

Definition 3.2 (Magnitude function). For a metric space (X, d) , we define its scaled version $tX := (X, d_t)$ by $d_t(x, y) := t \cdot d(x, y)$, where $t \in \mathbb{R}_+$ is the scaling factor. The *magnitude function* of (X, d) is the function $\text{Mag}_X : t \mapsto \text{Mag}(tX)$.

For $t \in (0, \infty)$, the magnitude function is defined for all but finitely many values of t (Leinster, 2013). The magnitude function is also *continuous* (Meckes, 2015, Corollary 5.5)¹ for negative definite metrics. Further, for finite metric spaces, we have $\lim_{t \rightarrow \infty} \text{Mag}(tX) = |X| = n$, i.e. the *cardinality* of X (Leinster, 2013, Proposition 2.2.6). This limit behaviour exemplifies to what extent the magnitude function describes the diversity of a space as ‘the effective number of points at scale t .’ Here, we extend magnitude functions to the domain $[0, \infty)$ by defining $\text{Mag}_X(0) := 1$.² Intuitively, this extension means that any metric space, when viewed from far away, looks like a single point. Notice that neither Definition 3.1 nor Definition 3.2 explicitly require specific properties of a metric (like the triangle inequality). Therefore, we find magnitude to be applicable even in the case of generalised similarity functions, including cosine similarity, provided the similarity matrix ζ_X is invertible.

¹The magnitude function is generally continuous for $t > t_{\text{crit}}$, where t_{crit} is the supremum of its finitely many singularities.

²This assumes the so-called *one-point property*, i.e. $\lim_{t \rightarrow \infty} \text{Mag}_X(0) = 1$, which was shown to hold generically for almost all finite metric spaces (Roff & Yoshinaga, 2023).

3.3. Magnitude for Evaluating Diversity

As a multi-scale geometric invariant, magnitude can be extended to evaluate the diversity of latent representations. Before elaborating on the specifics, we briefly describe our scenario. We assume that we are studying a set of latent representations \mathcal{X} , with each $X \in \mathcal{X}$ being a point cloud, i.e. $X \subseteq \mathbb{R}^D$. Given such a latent representation X , e.g. a text, image, or graph embedding, we can use the L^1 or L^2 distance as a meaningful metric; alternatively, even semi-metrics like the cosine distance can be employed. Based on the choice of metric, we can directly interpret $\text{Mag}_X(t)$ as the effective number of points at scale t . In practice, this summarises how diverse points in the space are when observed at said scaling factor. This multi-scale behaviour motivates us to propose a simple but expressive summary of a representation’s magnitude function.

Definition 3.3 (Area under the magnitude function, **MAGAREA**). Let X be a metric space whose magnitude function $\text{Mag}_X(t)$ has been evaluated across the interval $T = [t_1, t_i]$. We define the area under the magnitude function to be $\int \text{Mag}_X := \int_{t_1}^{t_i} \text{Mag}_X(t) dt$.

Moreover, we extend this proposed summary to measure the difference in diversity when comparing two representations generated by the *same* (embedding) model. Notice that distances in these spaces are directly comparable, implying that the respective magnitude functions can be compared across the same domain.

Definition 3.4 (Magnitude function difference, **MAGDIFF**). Let X and Y be two metric spaces that share the same notion of distance. Assume the associated magnitude functions $\text{Mag}_X(t)$ and $\text{Mag}_Y(t)$ have been evaluated across the same interval $T = [t_1, t_i]$. We define the magnitude function difference to be $\Delta \text{Mag}_{XY} := \int_{t_1}^{t_i} (\text{Mag}_X(t) - \text{Mag}_Y(t)) dt$.

Definition 3.3 and Definition 3.4 constitute novel multi-scale approaches for summarising and comparing magnitude functions, leading to theoretically well-founded diversity measures. As we will later demonstrate in our experiments, accumulating changes in magnitude across a *range* of scaling factors retains the desirable properties of single-scale magnitude, but yields more robust multi-scale summaries of diversity (see Appendix C for a theoretical and empirical investigation of stability to perturbations). Furthermore, this comparison in terms of the effective number of points across scales remains directly interpretable.

In practice, we *approximate* the integrals in Definition 3.3 and Definition 3.4 via numerical integration across evenly-spaced evaluation scales. Further, we obviate the choice of evaluation interval using knowledge about the convergence behaviour of magnitude functions. To do so, we define a magnitude function’s convergence scale:

Definition 3.5 (Convergence scale, t_{conv}). Given a magnitude function $\text{Mag}_X(t)$ define its approximate convergence scale as $t_{\text{conv}} \in \mathbb{R}$ such that $\text{Mag}_X(t_{\text{conv}}) = |X| - \epsilon$ for some small $\epsilon > 0$. We set $\epsilon := 0.05|X|$ in this work.

In practice, we find that *all* relevant changes in diversity happen at smaller scales of dissimilarity before magnitude functions flatten out and start increasing monotonically towards the cardinality of an input space. We thus choose t_i based on convergence scales, arguing that ‘nothing interesting’ happens at larger scales any more. We determine the convergence scale using numeric root finding procedures and use $t_1 := 0$ as a lower bound. As a consequence, our magnitude-based diversity measures do not require manual parameter selection. In terms of implementations, we also improve the efficiency of magnitude computations by using a Cholesky decomposition (see Appendix B for more details). Together with our automated scale selection procedure, we thus overcome the main hurdles that hitherto prevented the wider use of magnitude functions.

Practical usage. We briefly describe how to compute our magnitude metric for reference-free and reference-based diversity evaluation. First, when computing the intrinsic diversity of a single latent representation, we suggest computing $\text{MAGAREA}(t_{\text{cut}}) = \int_0^{t_{\text{cut}}} \text{Mag}_X(t) dt$ where $t_{\text{cut}} = t_{\text{conv}}$ is the estimated convergence scale. When computing the diversity for multiple embeddings *without* a reference dataset, we choose t_{cut} as the median convergence scale across all embeddings and compute $\text{MAGAREA}(t_{\text{cut}})$ as above. Taking the median here provides a stable compromise between the convergence behaviour of all functions. For *reference-based comparisons*, we compute the difference between the magnitude function of the reference and the generated data, once again taking a common convergence point to ensure a fair comparison. Specifically, for each latent representation X , we calculate our diversity metric $\text{MAGDIFF}(t_{\text{ref}}) = \int_0^{t_{\text{ref}}} \text{Mag}_X(t) - \text{Mag}_{\text{ref}}(t) dt$ from $t = 0$ until t_{ref} , i.e. the convergence scale of the reference. To evaluate the relative increase or decrease in magnitude we recommend normalising **MAGDIFF** either by the area under the reference function or by the cardinality of the space. As for the choice of the number of scales, we consider this to be a trade-off between *accuracy* and *computational performance*. For the text data, we select 65 evenly-spaced scales, for the image data 10, and, finally, for the graph data 40 scales, which we find reasonable given the size of each dataset. We also compute magnitude at one scale as a baseline, but the choice of scale here can depend vastly on the desired resolution. In general, we recommend choosing a scale less than or equal to the convergence scale and note that the higher the scale, the higher the sensitivity.

Limitations. The difference between magnitude functions is a reference-free measure of intrinsic diversity, which gives interpretable insights into changes in diversity, but does not measure *fidelity* and hence should not be interpreted in isolation, but jointly with coverage-based metrics when evaluating generative models, for instance. Moreover, while we speed up computational performance considerably, improved algorithms and approximation methods are needed to ensure that magnitude scales easily to hundreds of thousands of observations. Finally, our analysis is focused on evaluating representation-based diversity and we show that given a latent representation, magnitude is a better notion of diversity than current methods. However, we do not investigate whether embedding-based similarities outperform alternative task- or domain-specific similarities, leaving the choice of dissimilarity measure flexible.

4. Experiments

Our experimental suite demonstrates how magnitude leads to a better understanding of representational diversity. We show the following results:

- Magnitude functions capture the curvature of a space.
- Magnitude functions are interpretable measures of the diversity of embeddings, yielding superior results than other diversity measures when predicting the diversity of sentence embeddings across different text generating tasks and embedding models.
- Magnitude functions successfully detect mode dropping in simulated distributions of image, and graph embeddings, while also reliably detecting mode collapse in graph embeddings. They are superior to recall and coverage as measures of intrinsic diversity.

4.1. Magnitude Functions Summarise Geometry

Magnitude functions capture the ‘shape,’ i.e. the geometry that is characteristic of the intrinsic data manifold, by capturing curvature and diversity. Curvature estimation is an important task in numerous domains like computer vision, computational geometry, and computer-aided design. Previous works have shown that alternative multi-scale methods, such as *persistent homology*, are able to detect curvature (Bubenik et al., 2020; Turkes et al., 2022). Here, we demonstrate that the magnitude function is capable of achieving comparable performance, using simpler methods and only a single feature. To this end, we generate a balanced dataset of point clouds of different curvature, following the process described in Turkes et al. (2022) and detailed in Appendix E.1.

We first assess to what extent the magnitude function can detect whether a unit disk has positive or negative curvature. Our main observation from plotting the functions for both groups in Fig. 2 is that there is a clear separation between

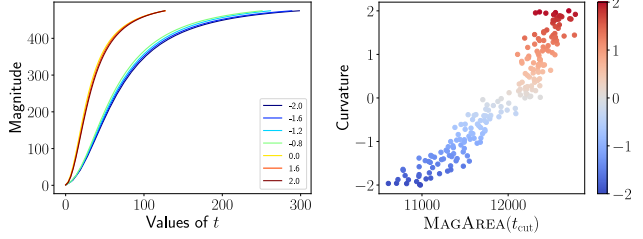


Figure 2. Magnitude detects curvature. Left: Magnitude functions for unit disks with curvature between $[-2, 2]$. Right: Curvature is positively correlated with our MAGAREA measure, indicating that it serves as a expressive predictor.

Table 1. Magnitude estimates curvature. Compared to more complex methods (Turkes et al., 2022), our measure MAGAREA performs best while only using a *single feature*.

METHOD	MSE (\downarrow)
SVR (selected PH features)	0.27 ± 0.07
SVR (PH vectorisation)	0.17 ± 0.05
SVR (all PH features)	0.16 ± 0.03
SVR (distance matrices)	0.24 ± 0.04
MLP (shallow)	1.15 ± 0.52
MLP (deep)	1.56 ± 0.68
MAGAREA (ours)	0.12 ± 0.04

Notation: PH: persistent homology features or vectorised representations; MLP: fully-connected neural network using pairwise distance matrices.

spaces of negative and positive curvature. We further test if we can predict the exact value of curvature (i.e. solve a regression task). To this end, we use quantile regression, using the area under the magnitude curve, MAGAREA, as a single feature. Using 5-fold cross validation, we achieve an MSE of 0.12 ± 0.04 , which improves on previous methods (Turkes et al., 2022) that made use of highly sophisticated topology-based features and more heavily-parametrised deep learning models (see Table 1 for more details). These results underscore the expressivity and power of magnitude-based metrics, which enable us to solve the *same* task with a highly-simplified model.

4.2. Magnitude Measures Diversity in Text Embeddings

We analyse data from Tevet & Berant (2021), consisting of 1K sets of 10 sentences each, generated for unique input prompts for 3 different sentence generation tasks, namely story completion (storyGen), dialogue response generation (respGen), and 3-word prompt completion (promptGen). Per task, 10 response sets have been generated using the same decoding parameter, the softmax-temperature dec, which controls the diversity and randomness of the generated text. Further, for 200 response sets per task,

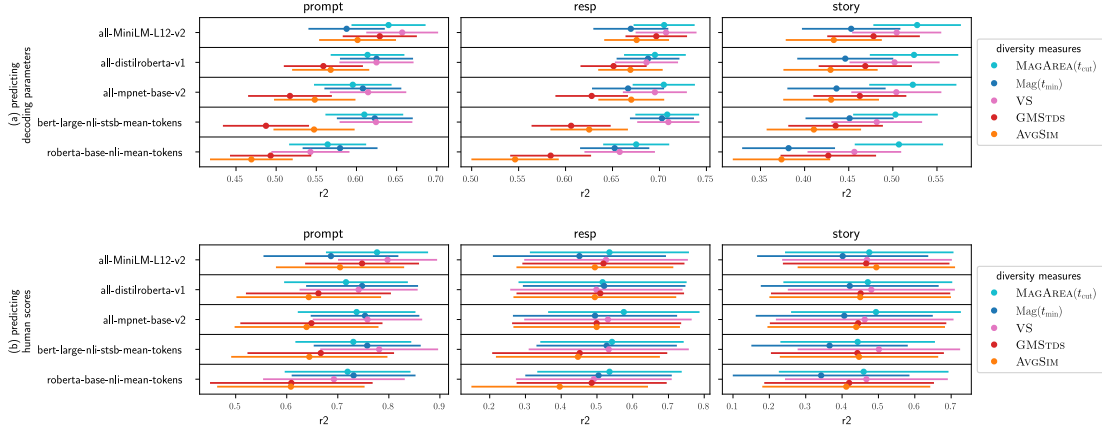


Figure 3. The area under the magnitude function outperforms alternative diversity measures at predicting (a) the decoding parameter, and (b) human evaluation scores, across 3 tasks and 5 embedding models. Baseline measures, AVGSIM and GMSTDS, perform noticeably worse. Points show the mean of the R^2 scores and lines the standard deviations across 5-fold cross-validation repeated 100 times.

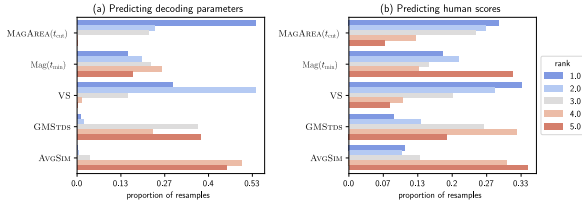


Figure 4. The area under the magnitude function outranks other diversity measures at (a) predicting decoding parameters and (b) predicting human-evaluated diversity scores across all experiments and cross-validation resamples.

mean human evaluation scores of text diversity were collected. We then embed each set of responses using 5 pre-trained sentence transformer models (Reimers & Gurevych, 2019), i.e. (1) ‘bert-large-nli-stsb-mean-tokens,’ (2) ‘roberta-base-nli-mean-tokens,’ (3) ‘all-mpnet-base-v2,’ (4) ‘all-distilroberta-v1,’ and (5) ‘all-MiniLM-L12-v2.’ For each dataset and model, we compute the area under the function $\text{MAGAREA}(t_{\text{cut}})$, evaluated until the median convergence scale across all functions, t_{cut} , and magnitude evaluated at the minimum convergence scale, $\text{Mag}(t_{\text{min}})$, computed using cosine distances. We compare this to the Vendi Score (VS), AVGSIM, and GMSTDS, calculated using cosine similarities. Moreover, we analyse the performance of each diversity metric at predicting the ground truth diversity scores, dec or ABSHDS, using 5-fold cross-validation repeated 100 times, trained via isotonic regression models;³ we report their performance in terms of the coefficient of determination, R^2 .

³We use these models because the relation between dec and diversity is likely monotonic, but not necessarily linear.

As a first step, we compute the mean Pearson and Spearman correlation between all diversity measures across all tasks and embeddings. This confirms that all notions of diversity agree in general with both rank and linear correlation above 0.9 on average. Overall, there is a slightly higher agreement between MAGAREA, Mag, and VS than between MAGAREA and AVGSIM or GMSTDS. Fig. 3 depicts results on the predictive performance of different diversity measures, while Fig. 4 shows summaries of the ranks achieved by each metric. We observe that in terms of R^2 scores, MAGAREA excels at predicting ground truth diversity, in particular for the story dataset, often outperforming VS (Fig. 3). Thus, even when taking the variability across resamples into account, there is no single dataset or embedding model for which either AVGSIM or GMSTDS can be considered preferable predictors of the ground truth softmax-temperature. Indeed, when predicting the decoding parameter, we find that MAGAREA consistently performs best, with median rank 1 across all experiments, followed by VS with a median rank of 2, Mag with median rank 3, and GMSTDS and AVGSIM sharing median rank 4 (Fig. 4, left). Thus, MAGAREA is most frequently the best-performing diversity measure across more than 50% of resamples, while VS most often achieves second place. The rankings of Mag are more varied supporting the observation that rather than considering diversity just at one single scale, MAGAREA yields a more robust, multi-scale summary of diversity. Results for predicting human scores (Fig. 4, right) follow the same general trends, but are more inconclusive due to the smaller sample size. Nevertheless, MAGAREA, Mag, and VS once again outperform the simpler summary statistics AVGSIM and GMSTDS. MAGAREA specifically is the best-performing diversity measure across this experiment.

Table 2. Magnitude performs well when predicting embedding models. We show the accuracy of different diversity scores for predicting embedding models, using a logistic regression classifier.

Dataset	MAGAREA	VS	GMSTDS	AVGSIM
cnn	0.86 ± 0.02	0.81 ± 0.03	0.29 ± 0.12	0.56 ± 0.08
patents	0.73 ± 0.07	0.63 ± 0.04	0.28 ± 0.11	0.46 ± 0.11
arXiv	0.77 ± 0.13	0.77 ± 0.02	0.30 ± 0.11	0.45 ± 0.11
bbc	0.83 ± 0.05	0.85 ± 0.03	0.30 ± 0.12	0.51 ± 0.11

4.3. Magnitude Distinguishes Embedding Models

Motivated by the capability of magnitude functions to encode representations, we now check whether the embedding spaces of different large language models can be inherently distinguished via their intrinsic structure. To this end, we embed 16384 documents of four different HuggingFace datasets, using five different models (see Appendix E.2 for more details). We further use PCA to reduce each embedding space to 384 dimensions to obtain a comparable dimensionality, subsampling 500 at random from each space, repeating this procedure 200 times. We then use logistic regression to predict the embedding based on the values of each diversity measure. Table 2 reports the results of 5-fold cross-validation with 20 repetitions. We observe that MAGAREA predicts the model with high accuracy. Further, it once again surpasses the performance and expressiveness of more naive summaries.

4.4. Magnitude Evaluates Image Embeddings

Mode dropping is a common issue in generative modelling, referring to the inability of a model to capture all parts of an input distribution (for instance, a model trained to generate images of animals suffers from mode dropping if it can only generate images of dogs). To simulate this, we randomly sample 200 images from each of the 10 classes in CIFAR10 and embed them using using a pre-trained Inception V3 model (Szegedy et al., 2016). Subsequently, we re-sample increasingly more observations from *one* preferred image class. We either drop modes sequentially, or we move the same number of observations simultaneously from all other classes. Importantly, diversity decreases gradually with the same ‘speed’ across both procedures, but fidelity should not change. We treat each class as preferred mode twice leading to 20 re-samples per mode dropping scenario (Naeem et al., 2020). Our analysis compares the changes in recall and coverage. Both of these metrics are calculated by setting the number of nearest neighbours to $k = 10$. Further, we calculate the change in $\text{Mag}(0.5)$, i.e. magnitude computed at the fixed scale $t = 0.5$, which we chose because it is roughly half of the convergence scale of the reference, relative to the magnitude of the reference. Similarly, $\text{MAGDIFF}(t_{\text{ref}})$ is taken as the difference between the magnitude functions relative to the area under the reference magnitude function.

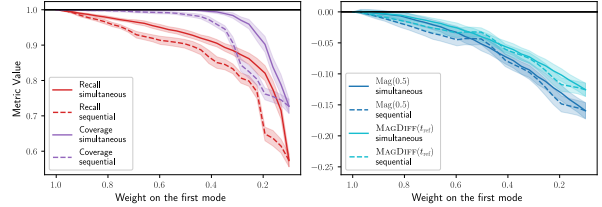


Figure 5. Magnitude detects the same decrease in diversity across simultaneous and sequential mode dropping. For both scenarios, the proportion of points on the first mode is plotted against recall, coverage, relative difference in magnitude at one scale and magnitude function difference relative to the reference.

Fig. 5 shows the changes in diversity as modes are being dropped. Ideally, every diversity measure should show the *same* decrease in diversity, irrespective of resampling strategy. However, we observe that current reference-based evaluation tools frequently fail to assert that diversity decreases in the same manner and at the same speed across both simultaneous and sequential mode dropping (Naeem et al., 2020). Indeed, both recall and coverage wrongly assess that diversity decreases faster during sequential resampling. Even worse, coverage only detects simultaneous mode dropping after around 70% of all points have shifted to one mode. This undesirable behaviour of both metrics is caused by their reliance on a fixed-neighbourhood size for manifold approximation resulting in an overestimate of the extent to which the perturbed samples reflect the diversity of the reference. In comparison, magnitude function difference between the reference and simulated data as well as magnitude evaluated at a single scale both successfully measure the gradual decrease in diversity across both mode dropping scenarios. Overall, across 20 re-samples, the mean decrease in magnitude is more highly correlated to the proportion of distorted points than to recall or coverage (Fig. 5). We also note that the trends shown by magnitude (even for a single scale) are generally steadier than the ones summarised by recall (or coverage), making magnitude difference a more purpose-built and reliable measure of diversity preservation.

4.5. Magnitude Evaluates Graph Generative Models

As previous works show, diversity evaluation in graph learning is fraught with difficulties, in particular when aiming to detect common problems like *mode collapse* or *mode dropping* (O’Bray et al., 2022; Thompson et al., 2022). In the following, we will study graph generative models (GGMs), which take a set of input graphs and generate new samples following the *same* distribution. The question that we aim to answer here is whether our proposed magnitude-based metric is more expressive in capturing the diversity of the generated graphs than classical metrics like *maximum mean discrepancy* (MMD) and metrics inspired from evaluat-

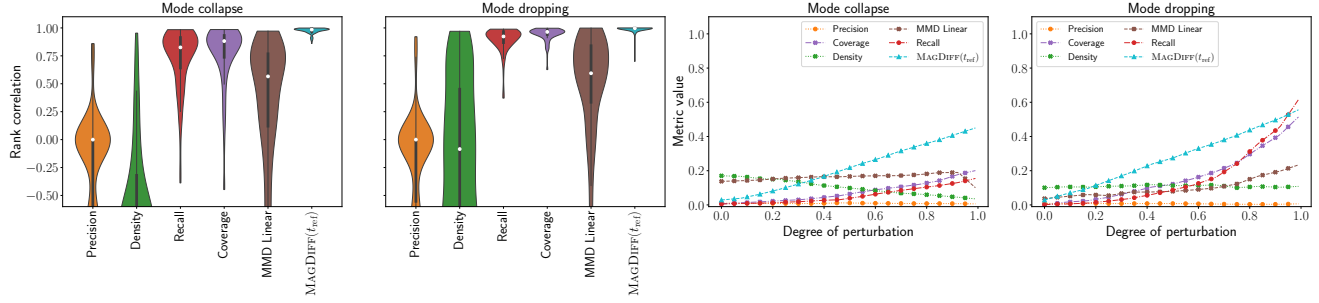


Figure 6. MAGDIFF outperforms all graph diversity metrics for mode collapse and mode dropping. Our magnitude-based metric detects mode collapse and mode dropping better than existing metrics for the Lobster dataset (the same pattern holds for Proteins, Community, Ego, Grid, see E.4). We report the Spearman correlation coefficient between each metric and the degree of perturbation p . Hence, the value of a metric that captures the decrease in diversity accurately should increase as a function of p , and rank correlation of 1 corresponds to an ideal metric. Our metric is the most sensitive to all changes in diversity for the mode collapse and the mode dropping experiment. It does well at capturing the change in diversity as measured by the degree of perturbation for values of p between $[0, 0.95]$.

ing image generative models (Precision, Recall, Coverage, Density). To this end, we analyse 3 synthetic (Lobster, Grid, and Community) and 2 real-world (Proteins and Ego) graph datasets, and compute multiple commonly used metrics for evaluating GGMs (O’Bray et al., 2022; Thompson et al., 2022) as detailed in Appendix E.4.

In order to test diversity of the generated samples, we follow the experimental setup of Thompson et al. (2022). For the *mode collapse* experiments, we substitute each point, i.e. each embedded graph, with its cluster centre, and thus the degree of perturbation p equals the proportion of clusters collapsed in this manner. The larger the value of p the more clusters have been collapsed. For the *mode dropping* experiments, we remove clusters, and keep the size of the generated dataset the same as the reference dataset by randomly resampling from the remaining classes. Again, the ratio p is the proportion of deleted clusters.

Fig. 6 shows the results of both *mode collapse* and *mode dropping* for the Lobster dataset. We observe similar trends across all datasets, but have chosen this dataset as a running example, following Thompson et al. (2022). An ideal measure should exhibit high rank correlation, indicating that they are capable of capturing the decrease in diversity properly, i.e. as a function of p . We note that in contrast to our magnitude-based metric, *Recall* and *Coverage* exhibit worse results, as evidenced by their lower mean correlation coefficient. Despite being specifically designed to measure the diversity of a dataset (Thompson et al., 2022), they only catch up to our magnitude metric when the degree of perturbation p is around 0.9 (see Fig. 6, right-hand plots). Magnitude dominates in the majority of the values of p , with recall and coverage being more sensitive for exceedingly large values of p , i.e. in unrealistic situations where most of the modes have been dropped. Moreover, their performance is highly contingent on k , the parameter used to construct a

k -NN graph. Please refer to Fig. 13 for aggregated results over all datasets, which exhibit a similar pattern in that our metric outperforms both *Recall* and *Coverage*.

5. Discussion

We have proposed novel diversity measures for evaluating latent representations. Our measures are based on *metric space magnitude*, a multi-scale invariant summarising geometrical characteristics of the input data. We have demonstrated axiomatically and empirically that our magnitude-based measures are superior to current baseline measures of intrinsic diversity. In a reference-free scenario, we observe that magnitude outperforms alternative measures when predicting the ground truth diversity for text embeddings. Given a reference dataset, we find that magnitude captures mode collapse and mode dropping better than existing metrics for evaluating generative models for both image and graph modalities. Furthermore, we have shown that magnitude can measure the intrinsic curvature of input data, outperforming previous methods. Magnitude thus gives a provably stable, unsupervised diversity metric that can be computed efficiently and allows users to flexibly choose a notion of dissimilarity.

For future work, we believe that magnitude exhibits a strong potential for applications to unaligned spaces with varying notions of distances. Further, we will explore connections between magnitude and other characteristic properties apart from curvature, studying e.g. the behaviour of magnitude as a way to assess overall geometric similarity in terms of the Gromov–Hausdorff distance (Mémoli, 2012). Moreover, we believe that integrating magnitude into deep learning models would be beneficial for obtaining novel diversity and geometry-based regularisation strategies.

Impact Statement

This paper presents work whose goal is to advance the evaluation diversity in representation learning, leading to increased fairness and trustworthiness in model evaluation. While representational diversity in terms of model outputs may have potential negative impacts, depending on the task at hand, we feel there are none that need to be specifically highlighted here. However, we acknowledge the potential for societal harm if our notion of representational diversity is confused with the meaning of diversity in the colloquial or societal context, which is admittedly even harder to measure and requires a larger discussion involving all affected communities.

Acknowledgements

K.L. is supported by the Helmholtz Association under the joint research school ‘Munich School for Data Science - MUDS.’ R.A. is supported by the United Kingdom Research and Innovation (grant EP/S02431X/1), UKRI Centre for Doctoral Training in Biomedical AI at the University of Edinburgh, School of Informatics and the International Helmholtz-Edinburgh Research School for Epigenetics (EpiCrossBorders). B.R. is supported by the Bavarian state government with funds from the *Hightech Agenda Bavaria*.

References

- Adamer, M. F., De Brouwer, E., O’Bray, L., and Rieck, B. The magnitude vector of images. *arXiv preprint arXiv:2110.15188*, 2021.
- Andreeva, R., Limbeck, K., Rieck, B., and Sarkar, R. Metric space magnitude and generalisation in neural networks. In Doster, T., Emerson, T., Kvinge, H., Miolane, N., Papillon, M., Rieck, B., and Sanborn, S. (eds.), *Proceedings of 2nd Annual Workshop on Topology, Algebra, and Geometry in Machine Learning (TAG-ML)*, volume 221 of *Proceedings of Machine Learning Research*, pp. 242–253. PMLR, 2023.
- Bubenik, P., Hull, M., Patel, D., and Whittle, B. Persistent homology detects curvature. *Inverse Problems*, 36(2): 025008, 2020.
- Bunch, E., Kline, J., Dickinson, D., Bhat, S., and Fung, G. Weighting vectors for machine learning: numerical harmonic analysis applied to boundary detection. *arXiv preprint arXiv:2106.00827*, 2021.
- Celikyilmaz, A., Clark, E., and Gao, J. Evaluation of text generation: A survey. *arXiv preprint arXiv:2006.14799*, 2020.
- Daly, A. J., Baetens, J. M., and De Baets, B. Ecological diversity: Measuring the unmeasurable. *Mathematics*, 6(7):119, 2018.
- Du, W. and Black, A. W. Boosting dialog response generation. In *Proceedings of the 57th Annual Meeting of the Association for Computational Linguistics*, 2019.
- Feragen, A., Lauze, F., and Hauberg, S. Geodesic exponential kernels: When curvature and linearity conflict. In *Proceedings of the IEEE Conference on Computer Vision and Pattern Recognition (CVPR)*, 2015.
- Friedman, D. and Dieng, A. B. The Vendi Score: A diversity evaluation metric for machine learning. *Transactions on Machine Learning Research*, 2023.
- Govc, D. and Hepworth, R. Persistent magnitude. *Journal of Pure and Applied Algebra*, 225(3):106517, 2021.
- Gretton, A., Borgwardt, K., Rasch, M., Schölkopf, B., and Smola, A. A kernel method for the two-sample-problem. *Advances in Neural Information Processing Systems*, 19, 2006.
- Higham, N. J. Cholesky factorization. *Wiley Interdisciplinary Reviews: Computational Statistics*, 1(2):251–254, 2009. doi: 10.1002/wics.18.
- Huntsman, S. Parallel black-box optimization of expensive high-dimensional multimodal functions via magnitude. *arXiv preprint arXiv:2201.11677*, 2022.
- Huntsman, S. Diversity enhancement via magnitude. In *International Conference on Evolutionary Multi-Criterion Optimization*, pp. 377–390. Springer, 2023.
- Kynkäänniemi, T., Karras, T., Laine, S., Lehtinen, J., and Aila, T. Improved precision and recall metric for assessing generative models. *Advances in Neural Information Processing Systems*, 32, 2019.
- Lai, Y.-A., Zhu, X., Zhang, Y., and Diab, M. Diversity, density, and homogeneity: Quantitative characteristic metrics for text collections. In Calzolari, N., Béchet, F., Blache, P., Choukri, K., Cieri, C., Declerck, T., Goggi, S., Isahara, H., Maegaard, B., Mariani, J., Mazo, H., Moreno, A., Odijk, J., and Piperidis, S. (eds.), *Proceedings of the 12th Language Resources and Evaluation Conference*, pp. 1739–1746, 2020.
- Leinster, T. The magnitude of metric spaces. *Documenta Mathematica*, 18:857–905, 2013.
- Leinster, T. *Entropy and Diversity: The Axiomatic Approach*. Cambridge University Press, 2021.

- Leinster, T. and Shulman, M. Magnitude homology of enriched categories and metric spaces. *Algebraic & Geometric Topology*, 21(5):2175–2221, 2021.
- Meckes, M. W. Positive definite metric spaces. *Positivity*, 17(3):733–757, 2013.
- Meckes, M. W. Magnitude, diversity, capacities, and dimensions of metric spaces. *Potential Analysis*, 42(2):549–572, 2015.
- Mémoli, F. Some properties of gromov–hausdorff distances. *Discrete & Computational Geometry*, 48(2):416–440, Sep 2012.
- Minc, H. *Nonnegative Matrices*. Wiley, New York, NY, USA, 1988.
- Naeem, M. F., Oh, S. J., Uh, Y., Choi, Y., and Yoo, J. Reliable fidelity and diversity metrics for generative models. In Daumé III, H. and Singh, A. (eds.), *Proceedings of the 37th International Conference on Machine Learning*, volume 119 of *Proceedings of Machine Learning Research*, pp. 7176–7185. PMLR, 2020.
- O’Bray, L., Horn, M., Rieck, B., and Borgwardt, K. Evaluation metrics for graph generative models: Problems, pitfalls, and practical solutions. In *International Conference on Learning Representations*, 2022.
- Reimers, N. and Gurevych, I. Sentence-BERT: Sentence embeddings using Siamese BERT-networks. In Inui, K., Jiang, J., Ng, V., and Wan, X. (eds.), *Proceedings of the 2019 Conference on Empirical Methods in Natural Language Processing and the 9th International Joint Conference on Natural Language Processing (EMNLP-IJCNLP)*, pp. 3982–3992. Association for Computational Linguistics, 2019.
- Roff, E. and Yoshinaga, M. The small-scale limit of magnitude and the one-point property. *arXiv preprint arXiv:2312.14497*, 2023.
- Sajjadi, M. S. M., Bachem, O., Lucic, M., Bousquet, O., and Gelly, S. Assessing generative models via precision and recall. In Bengio, S., Wallach, H., Larochelle, H., Grauman, K., Cesa-Bianchi, N., and Garnett, R. (eds.), *Advances in Neural Information Processing Systems*, volume 31. Curran Associates, Inc., 2018.
- Salim, S. *The q-spread dimension and the maximum diversity of square grid metric spaces*. PhD thesis, University of Sheffield, 2021.
- Simon, L., Webster, R., and Rabin, J. Revisiting precision recall definition for generative modeling. In Chaudhuri, K. and Salakhutdinov, R. (eds.), *Proceedings of the 36th International Conference on Machine Learning*, volume 97 of *Proceedings of Machine Learning Research*, pp. 5799–5808. PMLR, 2019.
- Solow, A. R. and Polasky, S. Measuring biological diversity. *Environmental and Ecological Statistics*, 1:95–103, 1994.
- Szegedy, C., Vanhoucke, V., Ioffe, S., Shlens, J., and Wojna, Z. Rethinking the inception architecture for computer vision. In *Proceedings of the IEEE Conference on Computer Vision and Pattern Recognition*, pp. 2818–2826, 2016.
- Tevet, G. and Berant, J. Evaluating the evaluation of diversity in natural language generation. In Merlo, P., Tiedemann, J., and Tsarfaty, R. (eds.), *Proceedings of the 16th Conference of the European Chapter of the Association for Computational Linguistics: Main Volume*, pp. 326–346. Association for Computational Linguistics, 2021.
- Theis, L., Oord, A. v. d., and Bethge, M. A note on the evaluation of generative models. In *International Conference on Learning Representations*, 2016.
- Thompson, R., Knyazev, B., Ghaleb, E., Kim, J., and Taylor, G. W. On evaluation metrics for graph generative models. In *International Conference on Learning Representations*, 2022.
- Turkes, R., Montufar, G. F., and Otter, N. On the effectiveness of persistent homology. In Koyejo, S., Mohamed, S., Agarwal, A., Belgrave, D., Cho, K., and Oh, A. (eds.), *Advances in Neural Information Processing Systems*, volume 35, pp. 35432–35448. Curran Associates, Inc., 2022.
- Xu, K., Hu, W., Leskovec, J., and Jegelka, S. How powerful are graph neural networks? In *International Conference on Learning Representations*, 2019.
- You, J., Ying, R., Ren, X., Hamilton, W., and Leskovec, J. Graphrnn: Generating realistic graphs with deep autoregressive models. In *International conference on machine learning*, pp. 5708–5717. PMLR, 2018.

A. Illustration of Magnitude and Magnitude Weights

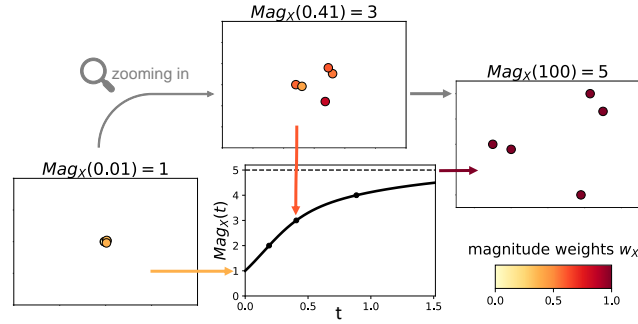


Figure 7. Example of magnitude weights and the magnitude function for a metric space with 5 points. When the scaling factor t is very small, e.g. $t = 0.01$, the magnitude weights of all points sum up to approximately 1, so that magnitude is very close to 1, and the space effectively looks like one point. Following this, as we zoom in further, magnitude grows and at $t = 0.41$, 3 distinct clusters or points are visible. Finally, for $t = 100$, all the points are clearly separated, their magnitude weights converge to one, and the value of magnitude approaches 5, i.e. the cardinality of the space.

While we did not use magnitude weights, which are the individual contribution of each point in a space to its overall magnitude, throughout our experiments, they play a more central role in some of the later proofs and the computation of magnitude in practice. Further, magnitude weights give an intuitive explanation on how each individual observation influences magnitude and the magnitude function as illustrated in 7.

Definition A.1 (Magnitude weights). Let $X = \{x_1, \dots, x_n\}$ be a finite metric space with an associated distance metric d . The similarity matrix of X is defined as $\zeta_X(i, j) = e^{-d(i, j)}$ for $1 \leq i, j \leq n$. If ζ_X is invertible, the magnitude weighting vector w_X is defined as $w_X := \zeta_X^{-1} \mathbb{1} = \mathbb{1}^\top \zeta_X^{-1}$. Denoting the i th element of w_X by w_{x_i} , we obtain an equivalent characterisation of magnitude as $\text{Mag}(X) = \sum_i w_{x_i}$.

B. Computing Magnitude

A naïve calculation of magnitude according to Definition 3.1 requires inverting the similarity matrix ζ_X , which has a worst-case complexity of $\mathcal{O}(n^3)$ and is numerically unstable. However, inverting ζ_X is not required in practice; instead, it suffices to solve certain linear equations as also pointed out by Huntsman (2022). First, we notice that the calculation of magnitude can be written as $\text{Mag}(X) := \mathbb{1}^\top \zeta_X^{-1} \mathbb{1}$. For finite metric spaces and negative definite metrics, ζ_X is a symmetric positive definite matrix, thus affording a Cholesky decomposition, which factorises $\zeta_X = LL^\top$, with L being a lower triangular matrix. This operation is numerically stable and more efficient than matrix inversion (Higham, 2009). We thus have $\text{Mag}(X) := \mathbb{1}^\top \zeta_X^{-1} \mathbb{1} = \mathbb{1}^\top (LL^\top)^{-1} \mathbb{1} = (L^{-1} \mathbb{1})^\top (L^{-1} \mathbb{1})$. This is equivalent to calculating $x^\top x$ with $x = L^{-1} \mathbb{1}$, which we can efficiently obtain by solving $Lx = \mathbb{1}$ since L is lower triangular. Likewise, we can reformulate the calculating of the magnitude weight vector $w_X = \zeta_X^{-1} \mathbb{1}$ as solving $\zeta_X w_X = \mathbb{1}$, which also benefits from the Cholesky factorisation.

To assess the improvements in computational efficiency, we benchmark the following computational methods in Python:

- Numpy inv: Inversion of the whole matrix ζ using `numpy.linalg.inv` as suggested by Bunch et al. (2021).
- Scipy solve: Solving for the magnitude weights using `scipy.linalg.solve` and assuming ζ to be positive definite.
- Cholesky weights: Cholesky decomposition using `scipy.linalg.cho_factor` to compute the magnitude weights.
- Cholesky: Using Cholesky decomposition as above to compute the value of magnitude directly
- Cg weights: Conjugate gradient iteration using `scipy.sparse.linalg.Cg` and an absolute tolerance of $1e-3$ to solve for the magnitude weights.
- Krylov weights: Pre-conditioned conjugate gradient iteration using `krypy.linsys.Cg` as implemented by Salim (2021) to solve for the weights.

All methods are evaluated on simulated data of a Swiss Roll with an increasing number of points. For each space, magnitude is evaluated at ten scales evenly spaced between zero and the convergence point. The computational times and their standard

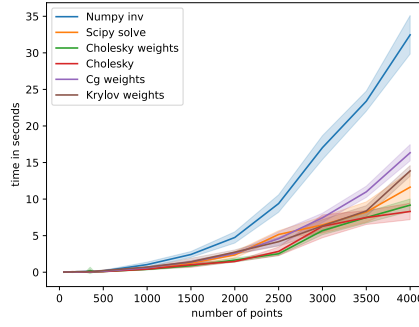


Figure 8. **Benchmark of computational times in seconds for magnitude functions evaluated across 10 scales.** We observe that Cholesky decomposition performs well, even for larger number of points. More efficient implementations may use information from previous steps to warm-start the solving procedure.

deviations are recorded across five re-runs in Figure 8. Results clearly show that naive inversion of the whole similarity matrix is by far the most costly method for computing magnitude. This is followed by the two conjugate gradient methods described above, where the pre-conditioned version is somewhat faster than the implementation without pre-conditioning for larger numbers of points. However, for evaluating magnitude at only 10 scales these approaches do not necessarily lead to improved performance compared to solving for the weights simply using `scipy.linalg.solve`. Finally, we note that our proposed implementation using Cholesky decomposition is the fastest computational method achieving less than a third of the computational time of the most naive implementation for larger datasets. Indeed, these results confirm that even for thousands of points magnitude is efficiently computable in a matter of seconds.

C. Stability of Magnitude

Next to the theoretical properties linking magnitude to geometrical properties of a space, which we previously outlined, we prove that magnitude, as a metric space invariant, also satisfies properties that are advantageous in the setting of analysing latent representations. Specifically, we prove that magnitude and thus the proposed magnitude differences satisfy certain *stability properties* in light of perturbations of metric space. By this, we mean that if two metric spaces X, Y are *close*, we want to obtain bounds on the differences between their magnitude values. The canonical choice to measure closeness would be the Gromov–Hausdorff distance, but in the absence of strong results concerning the behaviour of magnitude under this distance (Leinster, 2013), we resort to a more general—but also weaker—notation of similarity in terms of *continuity*. More precisely, we will show that the similarity matrices used in the calculation of magnitude are well-behaved in the sense that closeness of metric spaces (under some matrix norm) translates to a continuous bound on the variation of the similarity matrices. We first prove a general result about matrices and their associated transformations.

Lemma C.1. *Let $\|A\|_2 := \sup \{\|Ax\|_2 : x \in \mathbb{R}^n \text{ with } \|x\|_2 = 1\}$ refer to the induced 2-norm for matrices, and let A, B be two $n \times n$ matrices with $\|A - B\|_2 \leq \epsilon$. Moreover, let $f(M) := \mathbf{1}^\top M \mathbf{1}$. Then $\|f(A) - f(B)\|_2 \leq n\epsilon$.*

Proof. Because $\|\cdot\|_2$ is a *consistent* norm, we have $\|f(M)\|_2 \leq \|\mathbf{1}^\top\|_2 \|M\|_2 \|\mathbf{1}\|_2 = n\|M\|_2$ for all $n \times n$ matrices M . Without loss of generality, assume that $\|f(A)\|_2 \geq \|f(B)\|_2$ and $\|A\|_2 \geq \|B\|_2$. Thus, $\|f(A)\|_2 - \|f(B)\|_2 \leq d(\|A\|_2 - \|B\|_2) \leq d(\|A - B\|_2) = n\epsilon$. \square

Treating A, B as inverse similarity matrices, the preceding statement shows that if the two inverse similarity matrices are close with respect to their spectral radius, the difference between their magnitude can be bounded. The following lemma shows that the similarity matrices satisfy a general continuity condition.⁴

Lemma C.2. *Let (X, d_X) and (Y, d_Y) be two metric spaces with corresponding distance matrices D_X, D_Y and cardinality n . For all $\epsilon > 0$, there exists $\delta > 0$ such that if $|D_X - D_Y| < \delta$ holds elementwise, then $\|\zeta_X - \zeta_Y\|_2 \leq \epsilon$.*

⁴It is clear that the mapping itself is continuous because of the functions involved in its calculation. However, we find it important to remark on the bound obtained with respect to the *spectral norm* of the two similarity matrices.

Proof. As a consequence of the continuity of the exponential function, we know that there is δ such that $|\zeta_X - \zeta_Y| < n^{-1}\epsilon$. The row sums of $\zeta_X - \zeta_Y$ are therefore upper-bounded by ϵ . We thus have $\|\zeta_X - \zeta_Y\|_2 \leq \epsilon$ (Minc, 1988, Theorem 1.1, p. 24). \square

As a consequence of Lemma C.2, and the continuity of matrix inversion, we know that magnitude is well-behaved under small perturbations of the respective distance matrices. Given a pre-defined threshold ϵ , we can always find perturbations that preserve the magnitude difference accordingly. Notice that this result does not make any assumptions about the Gromov–Hausdorff distance of the metric space and only leverages the distance matrices themselves. Moreover, this result applies in case X, Y are close with respect to the *Hausdorff distance*. If $d_H(X, Y) < \delta$, the elementwise condition $|D_X - D_Y| < \delta$ is satisfied *a fortiori*. This stability of single-scale magnitude then further ensures the stability of the difference between magnitude functions as defined in 3.4 in the same sense. Nevertheless, from a theoretical point of view, this result could be made stronger by showing bounds in terms of distances between the metric spaces. We leave such a result for future work, noting in passing that such strong results remain elusive at the moment (Govc & Hepworth, 2021); it is known, however, that the magnitude function is at least *lower semicontinuous* (Meckes, 2013, Theorem 2.6).

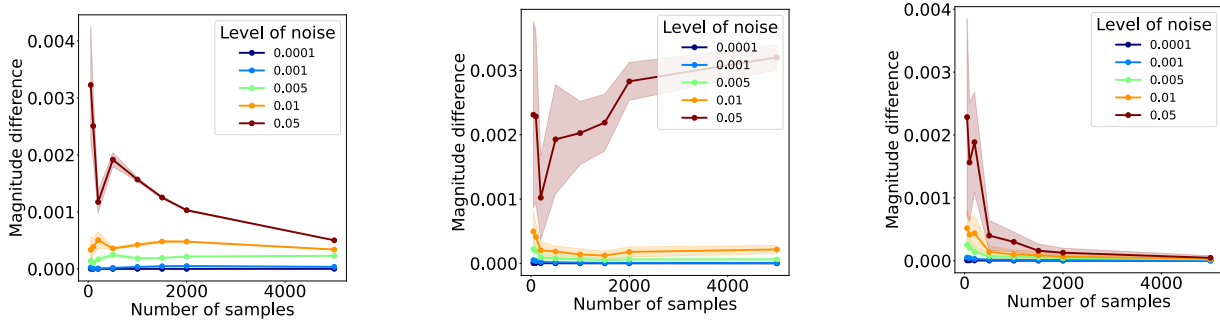


Figure 9. **Empirical stability of magnitude.** Magnitude difference is stable across different datasets (from left to right: Circles, Swiss Roll, Gaussian blobs) and sample sizes. The lines show the mean magnitude difference relative to the magnitude area of the unperturbed data and the shaded area the standard deviation calculated across 50 repetitions.

We further investigate the empirical stability of the magnitude function difference. Given the difficulty in proving strong theoretical stability results, we verify that, in practice, the magnitude function difference remains stable when adding noise to the input space. We thus sample points from a Laplace distribution with mean $\mu = 0$ and variance $2b^2$ with different levels of noise, i.e. $b \in \{0.0001, 0.001, 0.005, 0.01, 0.05\}$. Figure 9 depicts the errors in magnitude function difference relative to the area under the magnitude function of the unperturbed data across three different datasets (circles, Swiss Roll, Gaussian blobs), using a different number of samples (varying between 100 and 5000 across 50 repetitions). The bound of 5000 points has been chosen given the clear downwards trend across multiple noise levels; we expect the same trend to hold for larger sample sizes. We observe that the magnitude function difference does not increase above the value of 1×10^{-3} with increasing sample size. In fact, the difference fluctuates more for smaller number of points, but this is still within a very small range. We therefore conclude that the magnitude function difference between the original space and its noisy version does not change much, which indicates that our measure is reliable and stable across multiple experimental conditions.

D. Diversity Measures

D.1. Definitions of Intrinsic Diversity Measures

The difficulty in defining diversity in representation learning has lead to a few varying proposals for evaluating the intrinsic diversity of latent representations. Amongst these we consider the following three methods as baseline measures:

GMSTDS: For a X , a D -dimensional embedding, it is directly computed as

$$\text{GMSTDS} = \sqrt[D]{\prod_{i=j}^D \sigma_j} \quad (2)$$

where $\sigma_j = \sqrt{\frac{1}{n}(\sum_{i=1,\dots,n} x_{ij} - \hat{x}_j)^2}$ is the standard deviation across the j -th embedding dimension [Lai et al. \(2020\)](#). Thus, GMSTDS regards an embedding as a cluster and assessing diversity by quantifying its spread. Note that GMSTDS is not absence invariant and to avoid that problem in practice. Indeed, it always equals zero whenever one embedding dimension is constant. For our implementation in the experiments we thus choose ignore all constant embedding dimensions when computing GMSTDS.

AVGSIM: Average mean similarity (or variations of it) is the most frequently used diversity measure in ML. It is simply computed as

$$\text{AVGSIM} = \frac{1}{\binom{n}{2}} \sum_{i,j \leq n, j > i} \zeta(i, j) \quad (3)$$

across all distinct pairs of points in X assuming ζ is symmetric ([Tevet & Berant, 2021](#)). This approach simply summarises that in a more diverse space, observations should on average be less similar.

Vendi Score (VS): We also consider the Vendi Score, which is the only entropy-based diversity measure proposed in related ML literature. Let ζ be a positive semi-definite similarity matrix with $\zeta(i, i) = 1$ for all $i \leq n$. Compute λ_i , the eigenvalues of ζ/n . Then the Vendi Score is defined as

$$\text{VS} = \exp\left(-\sum_{i=1}^n \lambda_i \log(\lambda_i)\right) \quad (4)$$

taking $0 \log(0) = 0$ by convention. That is, the Vendi Score is the exponential of the Shannon entropy of the eigenvalues of ζ/n [Friedman & Dieng \(2023\)](#). It can thus be interpreted as summarising the effective number of modes in a space at a specific scale of similarity.

D.2. Defining Reference-based Evaluation Metrics

Here we define the metrics used in the image and graph embedding experiments.

$$\text{Precision} = \frac{1}{M} \sum_{j=1}^M 1_{Y_j \in \text{manifold}(X_1, \dots, X_N)} \quad (5)$$

$$\text{Recall} = \frac{1}{M} \sum_{i=1}^N 1_{X_i \in \text{manifold}(Y_1, \dots, Y_M)}, \quad (6)$$

where the manifold is defined as $\text{manifold}(X_1, \dots, X_N) = \bigcup_{i=1}^N B(X_i, \text{NND}_k(X_i))$. Here, $B(x, r)$ is the sphere in \mathbb{R}^d of radius r around x , and $\text{NND}_k(X)$ is the distance to the k -th nearest neighbour.

Similarly, Density and Coverage are defined as follows:

$$\text{Density} = \frac{1}{M} \sum_{j=1}^M \sum_{i=1}^N 1_{Y_j \in B(X_i, \text{NND}_k(X_i))}, \quad (7)$$

$$\text{Coverage} = \frac{1}{N} \sum_{i=1}^N 1_{\exists j s.t. Y_j \in B(X_i, \text{NND}_k(X_i))}, \quad (8)$$

Maximum Mean Discrepancy (MMD) [Gretton et al. \(2006\)](#); [You et al. \(2018\)](#) is a metric based on graph statistics. MMD Linear is computing MMD with a linear kernel ([O’Bray et al., 2022](#)). We define $\mathbb{S}_r = \{x_1^r, \dots, x_m^r\} \sim P_r$ and $\mathbb{S}_g = \{x_1^g, \dots, x_n^g\} \sim P_g$, where x_i is a feature vector from a corresponding graph G_i . Therefore, MMD is defined as follows:

$$\text{MMD}(\mathbb{S}_r, \mathbb{S}_g) = \frac{1}{m^2} \sum_{i,j=1}^m (k(x_i^r, x_j^r)) + \frac{1}{n^2} \sum_{i,j=1}^n (k(x_i^g, x_j^g)) - \frac{2}{nm} \sum_{i=1}^n \sum_{j=1}^m (k(x_i^g, x_j^r)), \quad (9)$$

where $k(\cdot, \cdot)$ is a general kernel function. For the case of the metric MMD Linear, used in our experiments, we use a linear kernel.

D.3. An Axiomatic Approach to Defining Intrinsic Diversity

The attempt to define, prove and interpret a theoretically well founded notion of diversity has inspired decades of heated debate in theoretical ecology. While in the context of machine learning, diversity is still very seldomly explored axiomatically, measures of biodiversity are often defined in a more well-established and unified framework built on mathematically complex ideas, such as entropy and extended notions of size. However, there is a lot of benefit to be gained by a more theoretical discussion on evaluating diversity in representation learning. Indeed, as pointed out by [Leinster \(2021\)](#), if a diversity measure does not pass basic logical tests, it is likely to be misleading and potentially useless for practical applications, which can have far-reaching detrimental consequences. By discussing some of these fundamental properties we thus uncover exactly how existing diversity measures for evaluating latent representations fail at essential requirements. We further discuss how magnitude functions improve upon alternative diversity metrics. Metric space magnitude as a diversity measure has been introduced with the following three properties fundamental properties in mind [Solow & Polasky \(1994\)](#):

- **Monotonicity in observations.** Including a new observation with all positive distances to a metric space with a negative definite metric does not decrease magnitude. Formally, for all $x_0 \notin X$ where (X, d) is a metric space define $(Z = X \cup x_0, d')$ via inclusion so that d' is a valid metric. Then if $d'(x_0, x) > 0$ for all $x \in X$, $\text{Mag}_X(t) \leq \text{Mag}_Z(t)$. This directly follows from Corollary 2.4. in [Leinster \(2013\)](#).
- **Twin property.** Magnitude does not change when including another identical observation already in the set. That is, for $x_0 \in X$ where (X, d) is a metric space, we get that $Z = x_0 \cup X = X$ and $\text{Mag}_Z(t) = \text{Mag}_X(t)$. This follows from the definition of a metric space because X is a set and cannot include duplicate observations.
- **Monotonicity in distances.** For $|Y| = |X| \geq 2$, when $f : (X, d_X) \mapsto (Y, d_Y)$ is a bijective mapping so that no distance is decreasing and at least distance is increasing and d_X and d_Y are negative definite, magnitude does not decrease. Formally, when $d_X(x_1, x_2) \leq d_Y(f(x_1), f(x_2))$ for all $x_1, x_2 \in X$ and $d_X(f(a), f(b)) < d_Y(f(a), f(b))$ for some $a, b \in X$, $\text{Mag}_X \leq \text{Mag}_Y$. Magnitude fulfils this property in particular for Euclidean spaces [Leinster \(2013\)](#).

Because these three essential properties hold for magnitude at every choice of t , they also hold for the are under the magnitude function for a space with a negative definite distance metric, whose magnitude function is necessarily continuous as demonstrated in Section C. However, none of the alternative diversity measures defined in Appendix D.1 fulfil the condition of being monotonic in observations. This can lead to an undesirable decrease in diversity when including novel observations to a space that adds information and should thus not reduce the total diversity, but is similar to existing points. Indeed, given this property we argue that a decrease in diversity as measured by the existing metrics can actually be misleading.

Further, elaborating on the idea that diversity measures should pass basic sanity checks, the following more basic properties are desirable for measuring the intrinsic diversity of a space as intended [Leinster \(2021\)](#):

- **Absence Invariant:** The diversity of a distribution when restricted to its support remains unchanged. It is invariant to the absence of observations.
- **Symmetry:** Diversity is invariant under permutations of the input observations.
- **Effective number:** Diversity should be measured in the range $[1, |X|]$, so diversity can be expressed as the effective number of distinct points in a space. When all observations are identical, diversity should equal 1. When all observations are completely dissimilar, diversity should be equal to the cardinality, $|X|$.

We note that the latter condition on diversity being measured as effective number is very helpful for measuring biodiversity [Daly et al. \(2018\)](#), but potentially not necessary in all applications. Nevertheless, symmetry and absence-invariance are key properties also when studying the diversity of latent representations. Indeed, symmetry is so essential that all diversity measures evaluated in this study fulfil it. GMSTDS however, is not absence invariant as it always equals zero whenever one feature or dimension in the embedding space is constant, which limits it's usefulness and makes it sensitive to the absence of information.

Finally, we note that diversity should be seen as a continuous function of the scale of similarity and behave accordingly:

- **Isometry invariance:** Diversity does not change under isometric transformations of a space.
- **Continuity:** Diversity is a continuous function of the similarity scale. Thus, diversity is not just a one-number summary, but a function of said scale.

D.4. Isometry Invariance of the Magnitude Function Difference

In the spirit of the discussion on intrinsic diversity in Appendix D.3 above, a measure of the difference in diversity between spaces should also fulfill certain desirable properties from both practical and theoretical perspectives. In the following we will show a minimum requirement, namely that the magnitude difference between isomorphic spaces equals zero.

Definition D.1 (Isometry). Let (X, d_X) and (Y, d_Y) be two metric spaces. A map $f: X \rightarrow Y$ is called an *isometry*, or distance-preserving, if for any $a, b \in X$, we have $d_X(a, b) = d_Y(f(a), f(b))$. X and Y are called *isometric* if there is a *bijective isometry* from X to Y .

Lemma D.2 (Isometry invariance). *Given two isometric spaces X, Y , we have $\text{Mag}_X = \text{Mag}_Y$.*

Proof. Let (X, d_X) and (Y, d_Y) be metric spaces with cardinality n and let $f: X \rightarrow Y$ denote their isometry. Then, the similarity matrix of X is $\zeta_{ij}^X = \exp(-d_X(a_i, a_j))$. Since f is an isometry, we have, $d_X(a_i, a_j) = d_Y(f(a_i), f(a_j))$. Hence, $\zeta_{ij}^X = \exp(-d_X(a_i, a_j)) = \exp(-d_Y(f(a_i), f(a_j))) = \zeta_{ij}^Y$. Since X and Y have the same similarity matrix, we have $\text{Mag}_X = \text{Mag}_Y$. \square

Corollary D.3. *The magnitude functions of two isometric spaces X, Y are equal for all $t \geq 0$.*

Notice that the *converse* of this statement is not true in general, i.e. there are non-isometric spaces whose magnitude functions are the same (Leinster, 2013).

Corollary D.4. *Let X be a metric space and $Y = cX$ with $c \in \mathbb{R}_+$. Then the magnitude functions of X and $1/cY$ are equal. Also, the magnitude functions of $1/\text{diam}_X X$ and $1/\text{diam}_Y Y$ are equal, where $\text{diam}_X := \max(d_X)$.*

Corollary D.5. *Magnitude function difference equals zero for isomorphic spaces.*

E. Experiments

In practice, we evaluate the integral Definition 3.4 using Trapezoidal integration across evenly spaced evaluation intervals. This formulation of difference then accumulates the total change in magnitude across their whole range of scaling factors. We also note that while the text embedding experiment is using cosine distances, all other experiments were evaluated using Euclidean distances. In the following we give further details and elaborate on the experimental setup and datasets used for our experiments as well as showcase extended results.

E.1. Curvature Experiments

Here we provide more details about the curvature experiments. We generate a unit disks D_κ of surfaces of constant curvature κ , with 3 cases: the first one is when $\kappa = 0$ (we then have the Euclidean plane), $\kappa < 0$ (we have a space of negative curvature, the Poincare disk model of the hyperbolic plane), $\kappa > 0$ (sphere with radius $1/\sqrt{\kappa}$). We vary the curvature κ to be in the interval $[-2, 2]$. For each value of κ , we construct point clouds by sampling 500 points from D_κ . We generate 201 surfaces with equally spaced curvature in the interval $[-2, 2]$.

Then, for the results reported in Table 1 we apply 5-fold cross-validation and first train a quantile regression model on the MAGAREA after applying polynomial feature transformation of degree 2 (this transformation is applied due to the quadratic-looking relationship between MAGAREA and curvature after exploratory analysis) computed for each space across 30 evenly spaced intervals until the scale $t_{\text{cut}} = 73$. We further reproduce six alternative models from Turkes et al. (2022). In particular, we use 0-dim PH simple (denoted by SVR (all PH features) in Table 1), which uses the lifespans of the Persistence Diagram computed on the samples; 0-dim PH simple 10 (SVR (selected PH features)) uses the 10 longest lifespans, and O-dim PH (SVR (PH vectorisation)), which selects the best PD vectorisation amongst a number of options (Persistence Images (PI), Persistence Landscapes (PL)). All the PH-based methods are followed by hyperparameter tuning of SVC with RBF kernel and choice of C parameters in $[0.001, 1, 100]$. We further compare to 3 methods based on pairwise distance matrices (denoted as ML, NN shallow and NN deep in Figure 4 of (Turkes et al., 2022); and as SVR(distance matrices), MLP (shallow) and MLP (deep) respectively in 1). We also note these models achieve different performance scores on our dataset then reported by Turkes et al. (2022) due to a slight difference in dataset and cross-validation splits. We ensure that all models are evaluated on the same splits of data in the 5-fold CV for fair comparison. Finally, we summarise the MSE achieved by each model in Table 1.

E.2. Text Experiments

We analyse data from [Tevet & Berant \(2021\)](#), consisting of 1K sets of 10 sentences each generated for unique input prompts for 3 sentence generation tasks. These tasks are story completion (storyGen) and dialogue response generation (respGen), both using MASS model fine-tuned on each dataset, and 3-word prompt completion (promptGen) using GPT-2-large without fine tuning. From the 1K response sets per task, 10 have been generated using the same decoding parameter, the softmax-temperature dec, sampled evenly across the range $[0.2, 1.2]$, which controls the trade-off between quality and diversity by skewing models towards avoiding low-probability tokens as dec decreases. This leads to potentially higher quality or fidelity but lower diversity or creativity in generated text. Further, for 200 of the 1K response per task, human workers rated the level of diversity of the response set on a scale from 5 (highest) to 1 (lowest). The mean of these scores, absolute HDS (ABSHDS), then measures the human perception of text diversity. In Figure 10 we further report the results when reproducing the experiment in Figure 3 using Euclidean instead of cosine distances. Vs is evaluated using the same similarity kernel as magnitude (see Definition 3.1). AvgSim is the average of these same similarities. AvDist is the average Euclidean distance and GMSTds is evaluated exactly as before.

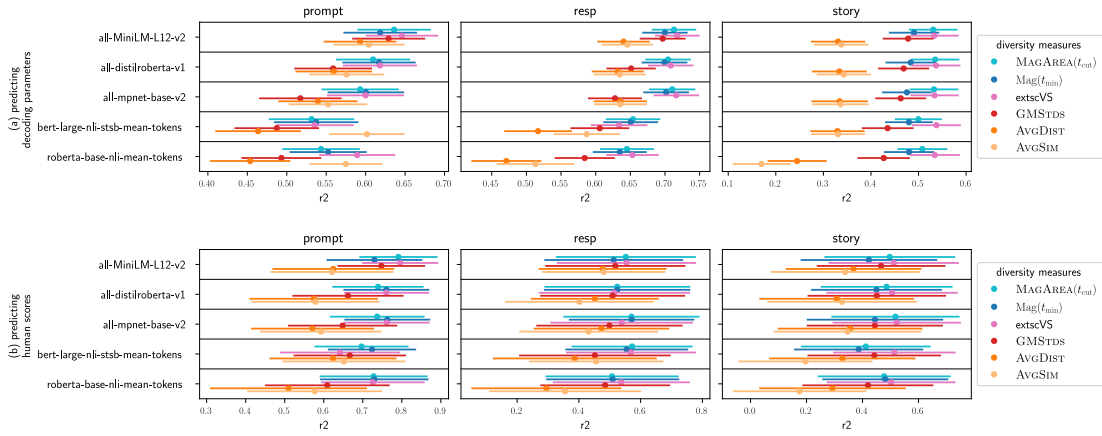


Figure 10. Prediction performance of diversity measures when either predicting (a) the ground truth soft-max temperature, DEC, or (b) human evaluation scores, ABSHDS, across 3 tasks and 5 embedding models using Euclidean distances. Mean of the R^2 scores and standard deviation across 5-fold cross-validation repeated 100 times.

For further experiments, we embed 16384 documents of four different HuggingFace datasets, CNN Dailymail, Patent, EdinburghNLP and Arxiv Abstracts, using five different models, (1) ada-002, (2) mistral-embed, (3) all-MiniLM-L6-v2, (4) all-distilroberta-v1, (5) all-mpnet-base-v2, and (6) multi-qa-distilbert-cos-v1. We then use PCA to reduce each embedding space to 384 dimensions to obtain a comparable dimensionality. This is done to mitigate some of the influence the difference in dimensionalities can have on the results of the analysis. Further, we sample 500 points at random from each space, repeating this procedure 200 times, which yields a dataset of 1000 embeddings generated by different models for each dataset. We further compute MAGAREA up to the median convergence point across all embeddings again using cosine distances. This is compare it to alternative diversity measures, VS, GMSTDS and AVGSIM computed as defined in Appendix D.1. For each dataset we then use multinomial logistic regression with L2 regularisation to classify the embedding model based on MAGAREA and report the mean and standard deviation of the accuracy across 5-fold cross-validation with 20 repetitions.

E.3. Image Experiments

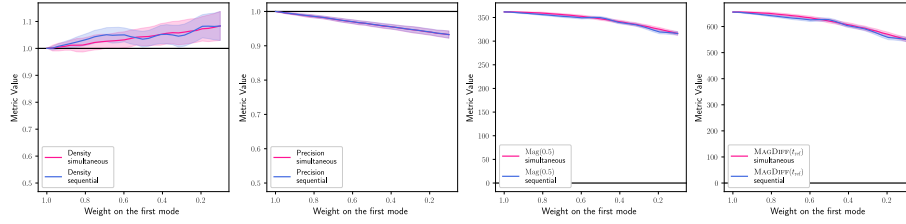


Figure 11. Line plots of the proportion of points on the first mode against recall, coverage, relative difference in magnitude at $t = 0.5$ and magnitude function difference relative to the reference across simultaneous sampling vs. sequential sampling.

In Figure 11 we further report the precision, density and the total difference in magnitude at one scale and the total difference in magnitude area for the same simulated mode dropping scenario as explained in the image embedding experiments.

E.4. Graph Embedding Experiments

More details on implementation. The metrics are normalised such that the value of each metric is 0 when $P_r = P_g$ (which is exactly when the degree of permutation is 0). Next, we vary the parameter p and compute each evaluation metric. We report the Spearman correlation coefficient between each metric and the degree of the perturbation p . Hence, the value of a metric which captures the decrease in diversity accurately should increase with the increase of p , and rank correlation of 1 corresponds to an ideal metric. For Precision, Recall, Density and Coverage we take the parameter $k = 5$.

The experimental setup used to evaluate the evaluation metrics for both mode collapse and mode dropping is as follows: First $P_r \approx P_g$, so that P_r , the real distribution, is identical to P_g , the generated distribution. Then the perturbation parameter $p \in [0, 1]$ is introduced, which transforms the generated graph datasets step-wise and increases the dissimilarity (and hence diversity) between the reference and generated datasets. Therefore, we use it as a proxy to measure the difference in diversity between P_r and P_g . We repeat the experiments for 5 different random seeds, 5 datasets, and GIN (Graph Isomorphism Network) (Xu et al., 2019) architectures as an embedding models (we vary the number of layers between $[2, 3, \dots, 7]$ and hidden dimensions (which we vary in the interval $[5, 30]$ with an increment of 5) for a total of 36 architectures.

Results for the whole experiment across all datasets are presented by Fig. 13.

Comparisons between different datasets. The magnitude metric can also be used to measure the intrinsic diversity between datasets. As a consistency check, we first compare if our metric can measure the relative diversity between the Grid and Lobster dataset. Indeed, the magnitude difference can detect that the Lobster dataset is more diverse than the Grid dataset as seen in Fig. 12.

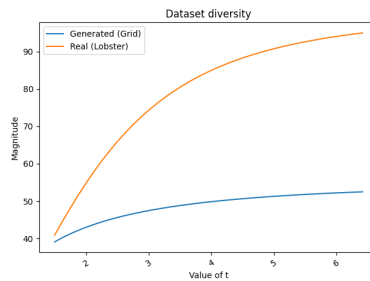


Figure 12. **Results from the Lobster and Grid datasets on intrinsic diversity of graphs** Here we demonstrate how our diversity metric can be used to detect which dataset has higher intrinsic diversity. We see that the Lobster dataset is more diverse by considering the area under the magnitude curves.

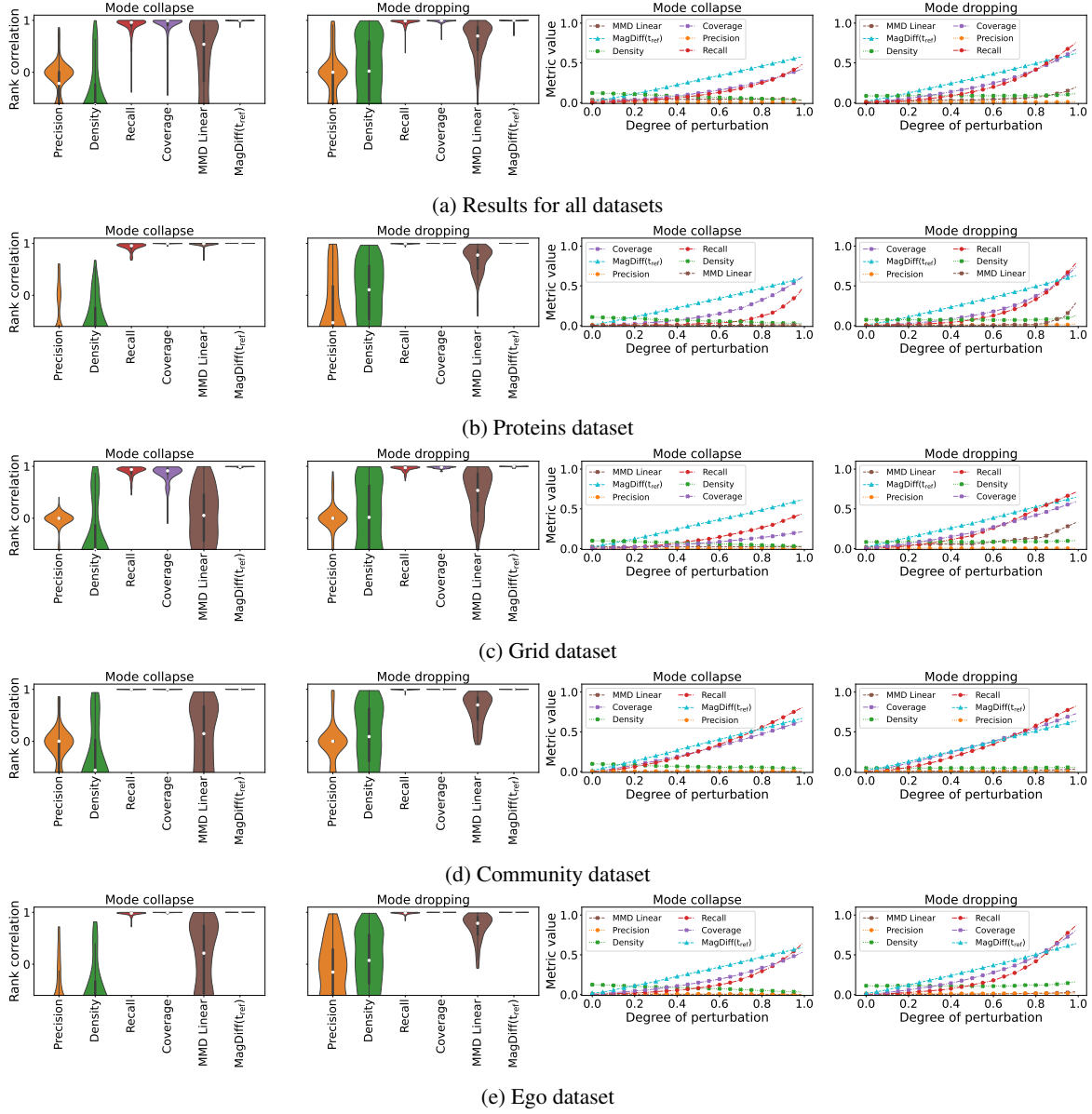


Figure 13. Results for the mode collapse and mode dropping experiments. The patterns for each of the datasets is similar to the results on the Lobster graphs, which we show in the paper.